PWNe beyond the free expansion

Authors: Rino Bandiera,
Niccolò Bucciantini,
Jonatan Martín (speaker),
Barbara Olmi
Diego F. Torres

First publication of a series

Monthly Notices of the ROYAL ASTRONOMICAL SOCIETY

MNRAS **499,** 2051–2062 (2020)
doi:10.1093/mnras/staa2956
Advance Access publication 2020 September 28

Reverberation of pulsar wind nebulae (I): impact of the medium properties and other parameters upon the extent of the compression

R. Bandiera,[1★] N. Bucciantini,[1,2,3] J. Martín,[4,5★] B. Olmi[1,4] and D. F. Torres[4,5,6★†]

[1] *INAF – Osservatorio Astrofisico di Arcetri, Largo E. Fermi 5, I-50125 Firenze, Italy*
[2] *Dipartamento de Fisica e Astronomia, Università degli Studi di Firenze, Via G. Sansone 1, I-50019 Sesto F. no (Firenze), Italy*
[3] *INFN – Sezione di Firenze, Via G. Sansone 1, I-50019 Sesto F. no (Firenze), Italy*
[4] *Institute of Space Sciences (ICE, CSIC), Campus UAB, Carrer de Can Magrans s/n, E-08193 Barcelona, Spain*
[5] *Institut d'Estudis Espacials de Catalunya (IEEC), Gran Capità 2-4, E-08034 Barcelona, Spain*
[6] *Institució Catalana de Recerca i Estudis Avançats (ICREA), E-08010 Barcelona, Spain*

Stay tuned for next papers!

Estimations regarding PWN detectability

- It is expected that PWNe will be the dominant gamma-ray sources detected by CTA (de Oña-Wilhelmi et al. 2013, Klepser et al. 2013, Abdalla et al. 2018)
- Current number of detected PWNe: **~34** (*TeVCat, http://tevcat.uchicago.edu/*)
- Estimated number in the first CTA Galactic Plane Survey: **~200**. Most of them have entered in the reverberation phase (*Fiori et al. 2022*)
- Most of the current radiative models in the literature simulate only the free expansion phase

Estimations regarding PWN detectability

- It is expected that PWNe will be the dominant gamma-ray sources detected by CTA (de Oña-Wilhelmi et al. 2013, Klepser et al. 2013, Abdalla et al. 2018)
- Current number of detected PWNe: **~34** (*TeVCat*, *http://tevcat.uchicago.edu/*)
- Estimated number in the first CTA Galactic Plane Survey: **~200**. Most of them have entered in the reverberation phase (*Fiori et al. 2022*)
- Most of the current radiative models in the literature simulate only the free expansion phase

We need a better understanding and modelling of the reverberation phase to characterise the PWN population correctly.

Estimations regarding PWN detectability

- It is expected that PWNe will be the dominant gamma-ray sources detected by CTA (de Oña-Wilhelmi et al. 2013, Klepser et al. 2013, Abdalla et al. 2018)
- Current number of detected PWNe: **~34** (*TeVCat*, http://tevcat.uchicago.edu/)
- Estimated number in the first CTA Galactic Plane Survey: **~200**. Most of them have entered in the reverberation phase (*Fiori et al. 2022*)
- Most of the current radiative models in the literature simulate only the free expansion phase

We need a better understanding and modelling of the reverberation phase to characterise the PWN population correctly.

What is the impact of the ejecta profiles on the compression of the PWN?

Evolution equations

$$\frac{dR}{dt} = v(t)$$

$$\frac{dM}{dt} = 4\pi R^2(t)\rho_{ej}(R,t)\left[v(t) - v_{ej}(R,t)\right]$$

$$\frac{d}{dt}[M(t)v(t)] = F(t) \text{ being } F(t) = 4\pi R^2(t)[P_{\rm pwn}(t) - P_{\rm ej}(R,t)] + \frac{dM}{dt}v_{\rm ej}(R,t)$$

The internal energy E_{pwn} is calculated by integrating the electron-positron distribution function in energy and the pressure is given by

$$P_{\rm pwn}(t) = \frac{3(\gamma_{\rm ad} - 1)E_{\rm pwn}}{4\pi R^3_{\rm pwn}(t)}$$

Evolution equations

$$\frac{dR}{dt} = v(t)$$

$$\frac{dM}{dt} = 4\pi R^2(t)\rho_{ej}(R,t)[v(t) - v_{ej}(R,t)]$$

$$\frac{d}{dt}[M(t)v(t)] = F(t) \text{ being } F(t) = 4\pi R^2(t)[P_{\rm pwn}(t) - P_{\rm ej}(R,t)] + \frac{dM}{dt}v_{\rm ej}(R,t)$$

How is the compression and re-expansion of the PWN when we vary these profiles?

The internal energy E_{pwn} is calculated by integrating the electron-positron distribution function in energy and the pressure is given by

$$P_{\rm pwn}(t) = \frac{3(\gamma_{\rm ad} - 1)E_{\rm pwn}}{4\pi R^3_{\rm pwn}(t)}$$

SNR profiles

Forward and reverse shock trajectories (Truelove & McKee 1999)

Updated version in **Bandiera et al. 2022, MNRAS, 508, 3194**

Unshocked profiles (Blondin et al. 2001)

$$v_{\rm ej}(r,t) = \frac{r}{t} \qquad P_{\rm ej}(r,t) = 0$$

$$\rho_{\rm ej}(r,t) = \begin{cases} A/t^3, & \text{if } r < v_t t \\ A(v_t/r)^{\omega} t^{\omega-3}, & \text{if } v_t t < r < R_{\rm rs} \end{cases}$$

Shocked profiles (Bandiera 1984)

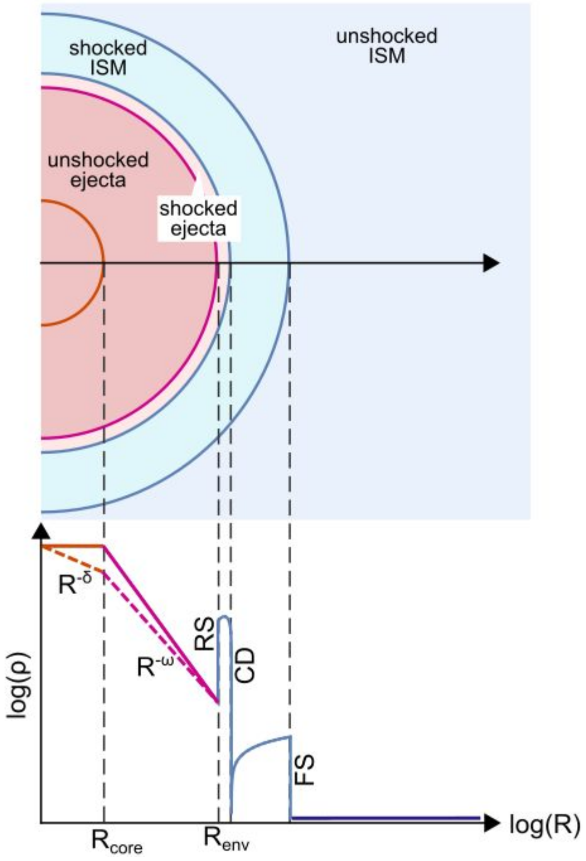

SNR profiles

Forward and reverse shock trajectories (Truelove & McKee 1999)

Updated version in **Bandiera et al. 2022, MNRAS, 508, 3194**

Unshocked profiles (Blondin et al. 2001)

$$v_{\rm ej}(r,t) = \frac{r}{t} \qquad P_{\rm ej}(r,t) = 0$$

$$\rho_{\rm ej}(r,t) = \begin{cases} A/t^3, & \text{if } r < v_t t \\ A(v_t/r)^{\omega} t^{\omega-3}, & \text{if } v_t t < r < R_{\rm rs} \end{cases}$$

SNR envelope density index

Shocked profiles (Bandiera 1984)

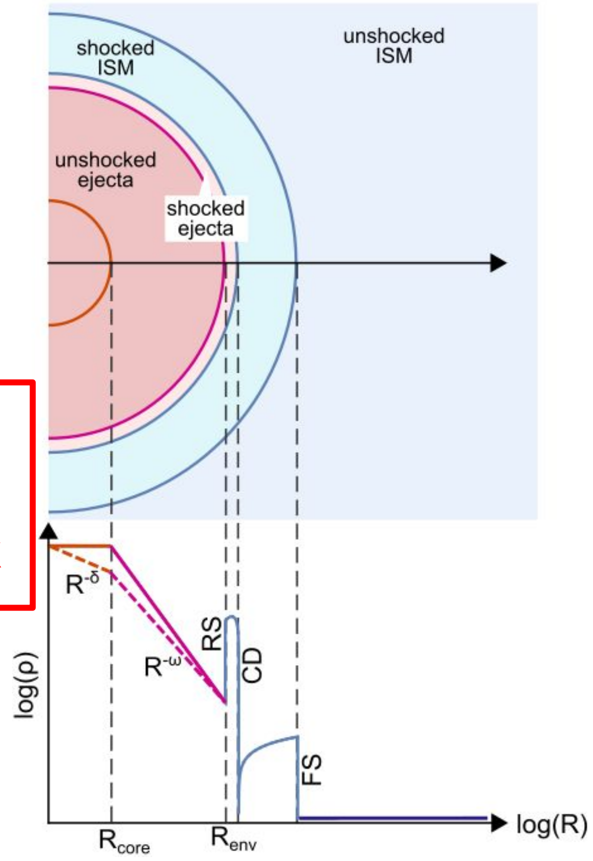

Simulation parameters

The equations are solved by using TIDE (Martin et al. 2012, Torres et al. 2014, Martin et al. 2016)

Parameter	Symbol	Crab Nebula	J1834.9−0846
Braking index	n	2.51	2.2
Initial spin-down age (yr)	τ_0	758	280
Initial spin-down luminosity (erg s^{-1})	L_0	3×10^{39}	1.74×10^{38}
SNR ejected mass ($M_\odot$)	M_{ej}	9	11.3
Far-infrared temperature (K)	T_{fir}	70	25
Far-infrared energy density (eV cm^{-3})	w_{fir}	0.1	0.5
Near-infrared temperature (K)	T_{nir}	5000	3000
Near-infrared energy density (eV cm^{-3})	w_{nir}	0.3	1
Energy break	γ_b	$9 \cdot 10^5$	10^7
Low energy index	α_l	1.5	1
High energy index	α_h	2.54	2.1
Containment factor	ϵ	0.27	0.6
Magnetic fraction	η	0.02	0.045

CF with the SNR envelope density index

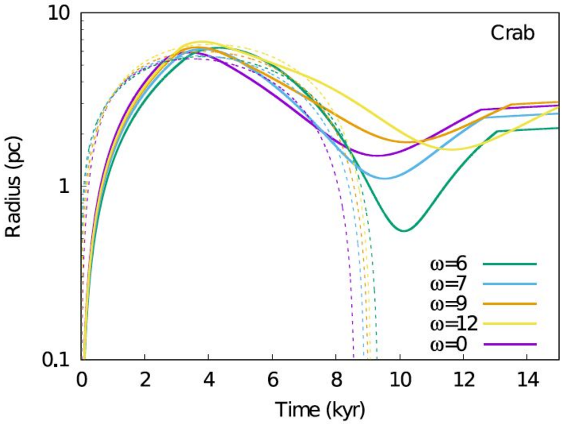

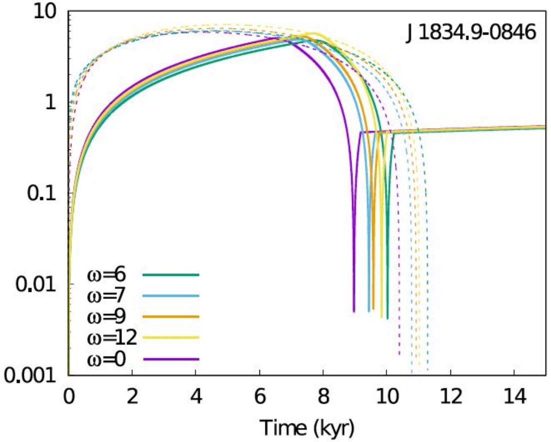

Compression factor

$$CF = \frac{R_{\max}}{R_{\min}}$$

	$w=0$	$w=6$	$w=7$	$w=9$	$w=12$
Crab Nebula					
$R_{\max}$ (pc)	5.912	6.281	6.177	6.329	6.816
$R_{\min}$ (pc)	1.499	0.551	1.106	1.793	1.626
CF	3.944	11.40	5.585	3.530	4.192
J1834.9−0846					
$R_{\max}$ (pc)	5.041	4.765	4.902	5.270	5.676
$R_{\min}$ (pc)	0.005	0.004	0.005	0.005	0.004
CF	1008	1191	980.4	1054	1419

CF with the SNR envelope density index

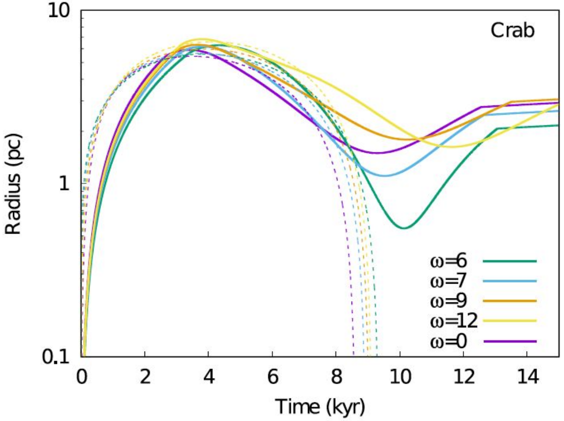

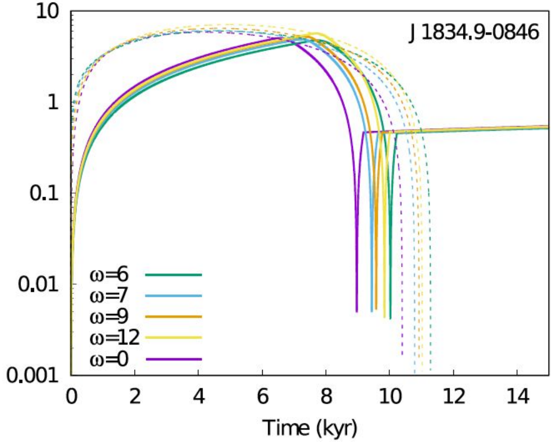

Compression factor

$$CF = \frac{R_{\rm max}}{R_{\rm min}}$$

No-monotonic behaviour of the CF. Complex physics behind need to be studied deeper (Bandiera et al. 2022, in prep.)

	$w = 0$	$w = 6$	$w = 7$	$w = 9$	$w = 12$
Crab Nebula					
$R_{\rm max}$ (pc)	5.912	6.281	6.177	6.329	6.816
$R_{\rm min}$ (pc)	1.499	0.551	1.106	1.793	1.626
CF	3.944	11.40	5.585	3.530	4.192
J1834.9−0846					
$R_{\rm max}$ (pc)	5.041	4.765	4.902	5.270	5.676
$R_{\rm min}$ (pc)	0.005	0.004	0.005	0.005	0.004
CF	1008	1191	980.4	1054	1419

Shocked ejecta pressure is a key parameter

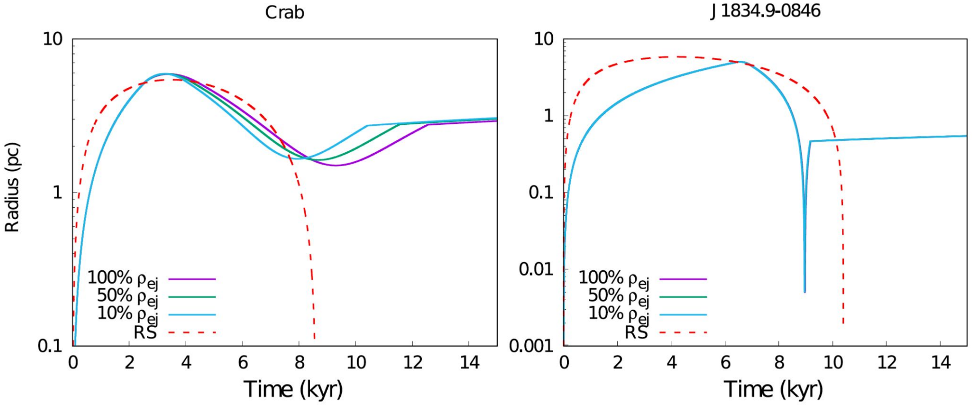

$$\omega = 9$$

We manually modify the density, velocity and pressure profiles to see their influence in the evolution of the radius.

For density, small differences in Crab-like and imperceptible in J1834-like PWNe

Shocked ejecta pressure is a key parameter

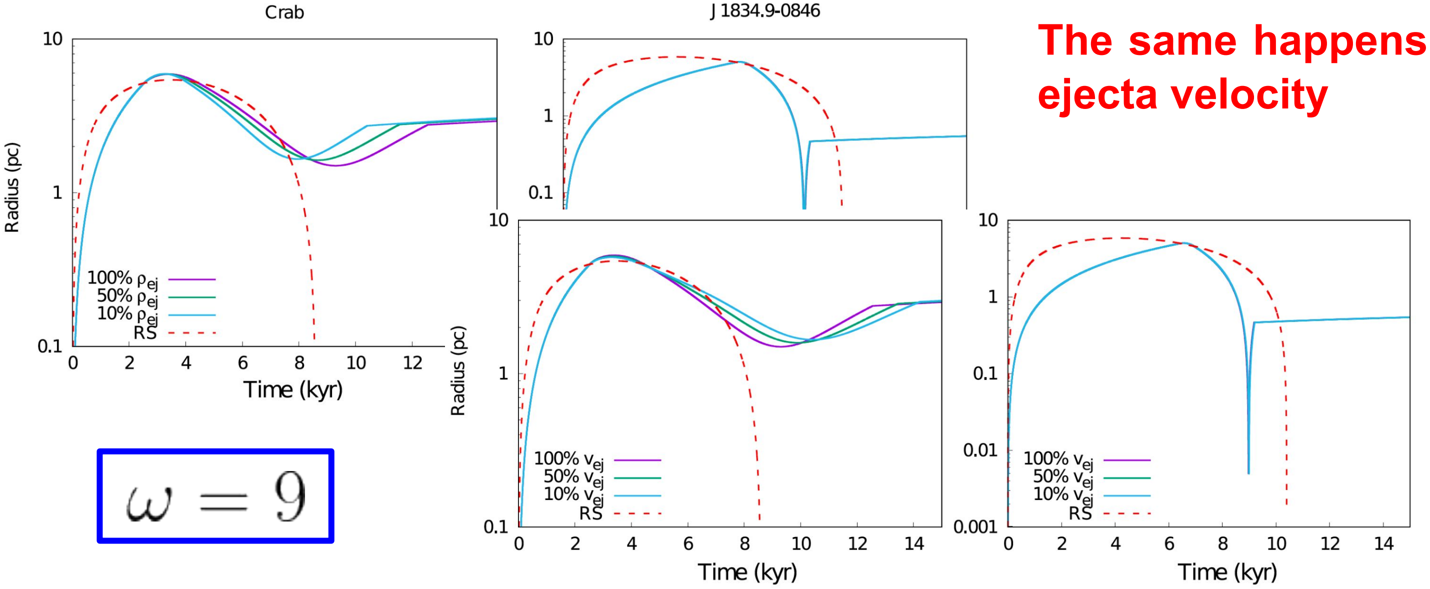

The same happens when we vary the ejecta velocity

$$\omega = 9$$

Shocked ejecta pressure is a key parameter

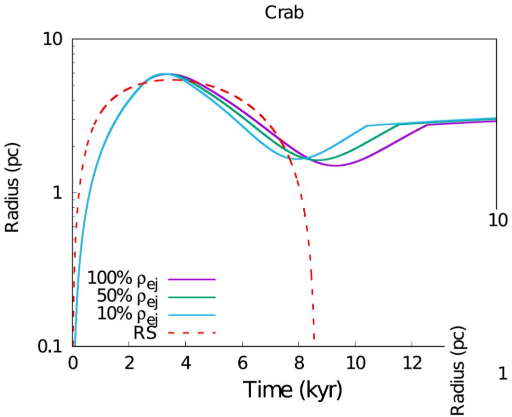

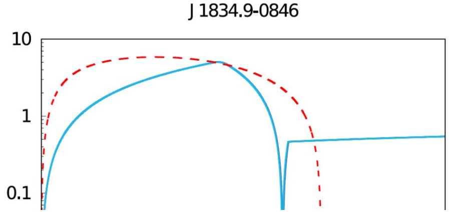

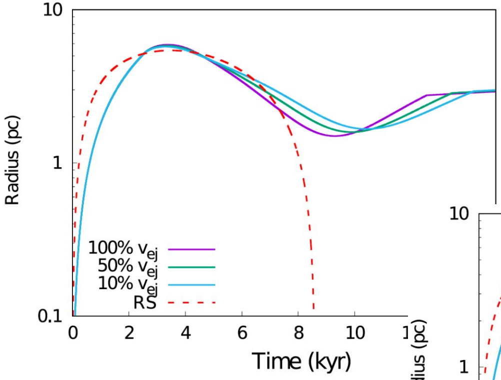

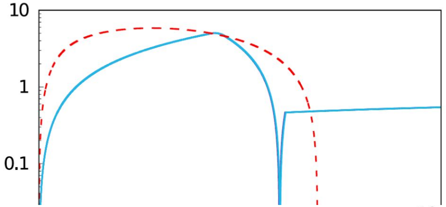

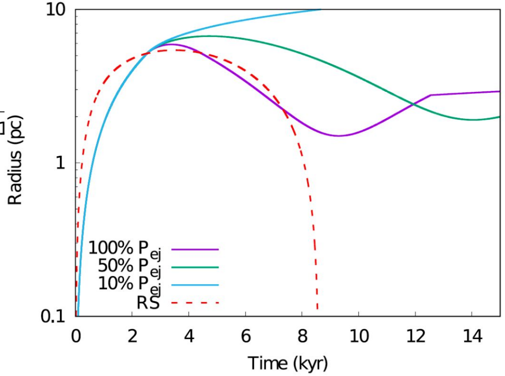

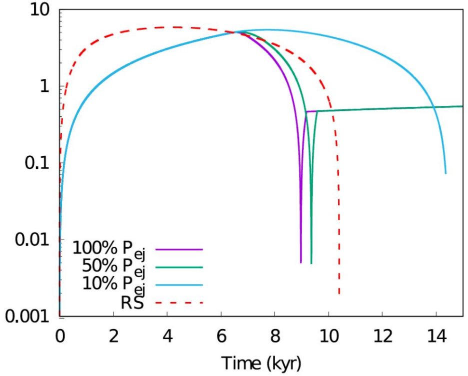

Clearly, the ejecta pressure makes the difference

$$\omega = 9$$

Same effects in the mass of the PWN shell

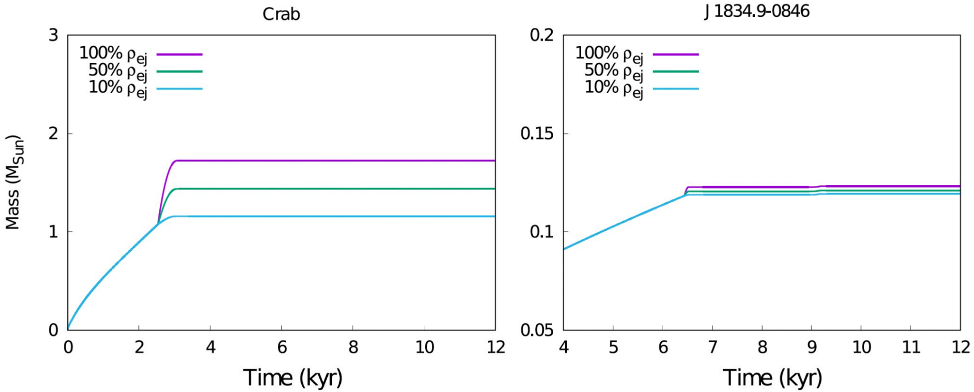

$$\omega = 9$$

Same effects in the mass of the PWN shell

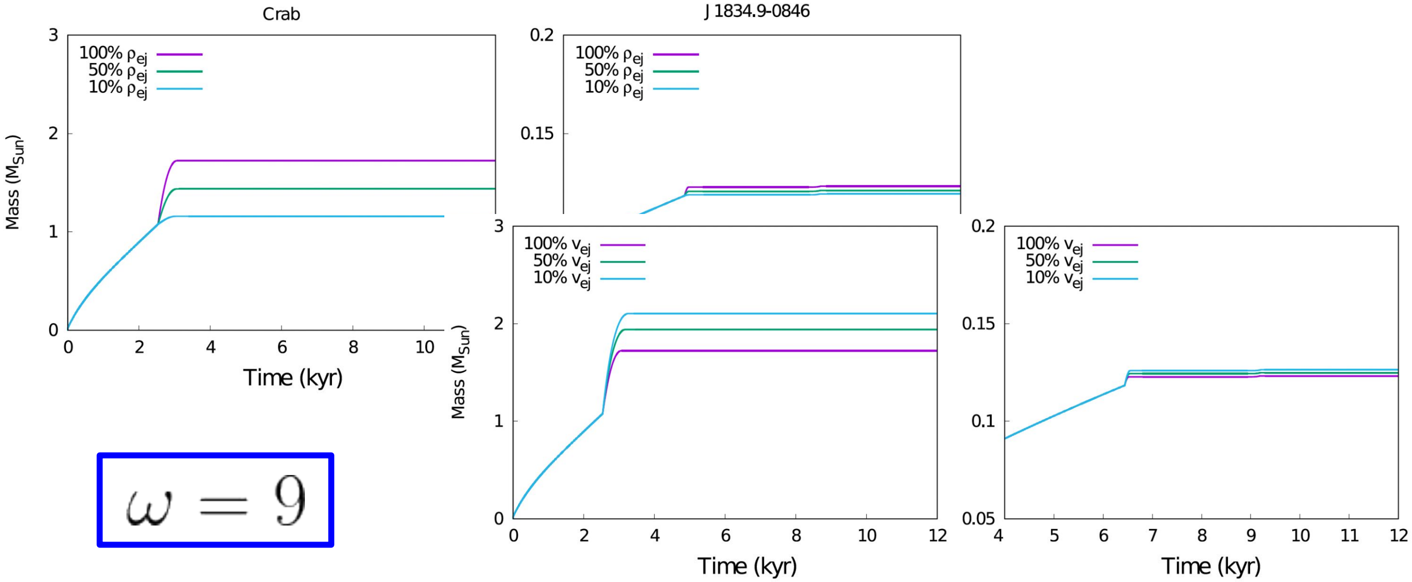

$$\omega = 9$$

Same effects in the mass of the PWN shell

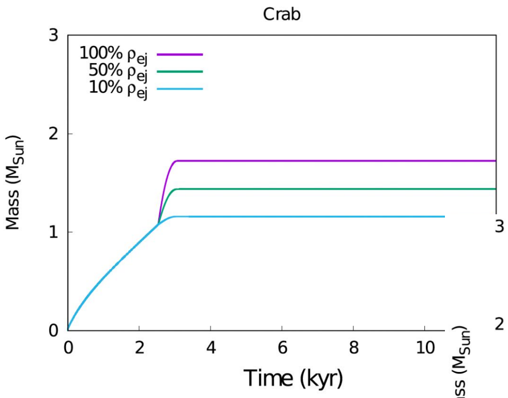

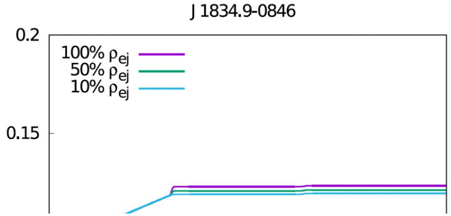

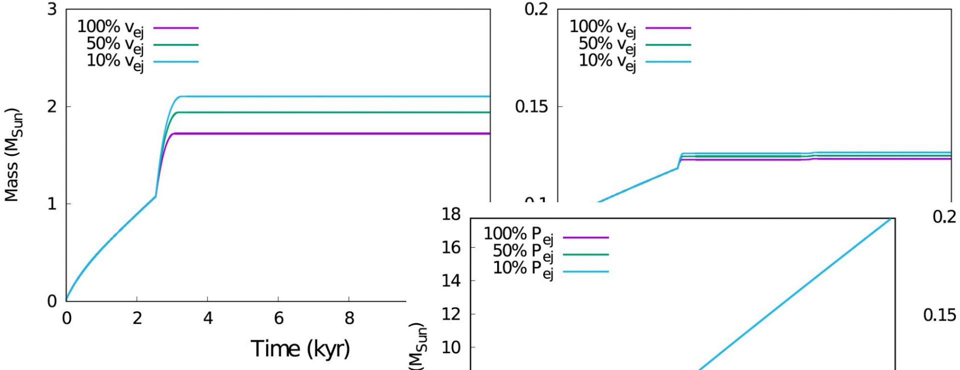

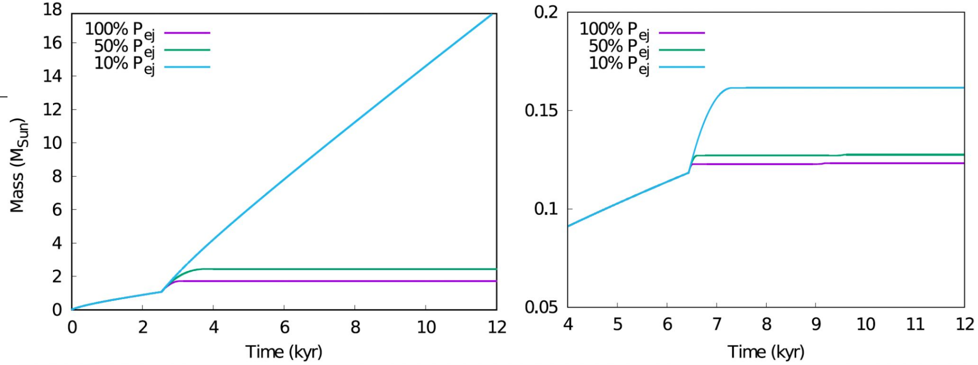

$$\omega = 9$$

Radiative vs. Non-radiative models

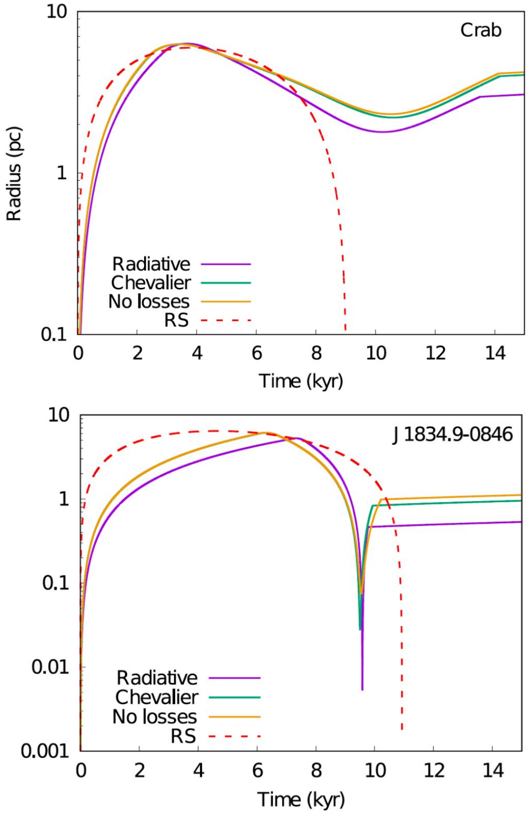

$\omega = 9$

Green line: equations from Chevalier et al. 2005

	Radiative	Chevalier	No losses
Crab Nebula			
R_{max} (pc)	6.329	6.274	6.274
R_{min} (pc)	1.793	2.204	2.313
CF	3.530	2.847	2.712
J1834.9−0846			
R_{max} (pc)	5.270	6.121	6.137
R_{min} (pc)	0.005	0.028	0.076
CF	1054	218.6	80.75

Radiative vs. Non-radiative models

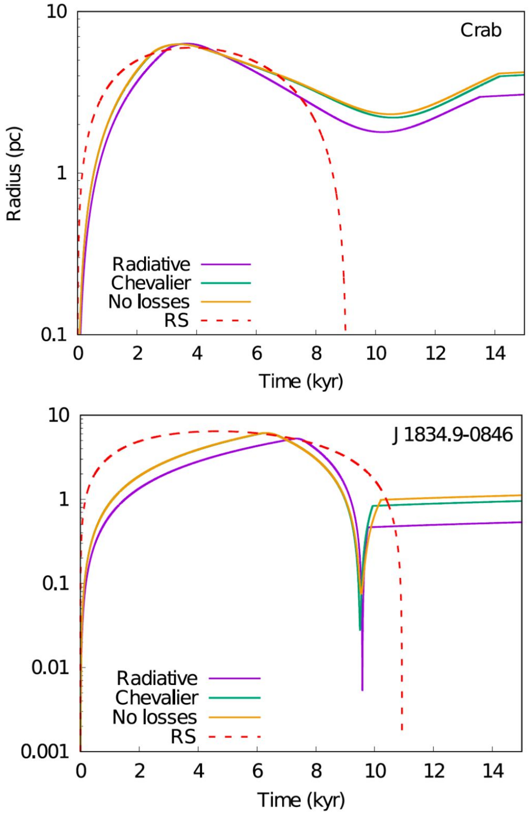

$\omega = 9$

	Radiative	Chevalier	No losses
Crab Nebula			
$R_{\rm max}$ (pc)	6.329	6.274	6.274
$R_{\rm min}$ (pc)	1.793	2.204	2.313
CF	3.530	2.847	2.712
J1834.9−0846			
$R_{\rm max}$ (pc)	5.270	6.121	6.137
$R_{\rm min}$ (pc)	0.005	0.028	0.076
CF	1054	218.6	80.75

CF increases significantly when we take into account radiative losses

Conclusions

- PWN radius evolution is very sensitive to the ejecta pressure profile. The same happens with the mass of the shell
- The consideration of radiation losses increases the CF significantly. In low spin-down luminosity cases there can be large differences (factors ~10)
- It is crucial to find a good representation of the ejecta pressure in order to get radiative models compatible with the results obtained in HD simulations
- We showed that the assumption of the bounding SNR to be in a relaxed Sedov state must be handled with care. A more appropriate description of the SNR properties will be discussed in the forthcoming papers of the same series